

Wounding Induces Facultative *Opn5*-Dependent Circadian Photoreception in the Murine Cornea

Nicolás M. Díaz,¹ Richard A. Lang,²⁻⁵ Russell N. Van Gelder,^{1,6} and Ethan D. Buhr¹

¹Department of Ophthalmology, University of Washington School of Medicine, Seattle, Washington, United States

²Center for Chronobiology, Cincinnati Children's Hospital Medical Center, Cincinnati, Ohio, United States

³The Visual Systems Group, Abrahamson Pediatric Eye Institute, Cincinnati Children's Hospital Medical Center, Cincinnati, Ohio, United States

⁴Division of Pediatric Ophthalmology, Cincinnati Children's Hospital Medical Center, Cincinnati, Ohio, United States

⁵Department of Ophthalmology, University of Cincinnati, College of Medicine, Cincinnati, Ohio, United States

⁶Department of Biological Structure and Pathology, University of Washington School of Medicine, Seattle, Washington, United States

Correspondence: Ethan D. Buhr, Department of Ophthalmology, Campus Box 358058, University of Washington School of Medicine, 750 Republican Street, Seattle, WA 98109, USA; buhre@uw.edu.

Received: April 3, 2020

Accepted: May 4, 2020

Published: June 16, 2020

Citation: Díaz NM, Lang RA, Van Gelder RN, Buhr ED. Wounding induces facultative *Opn5*-dependent circadian photoreception in the murine cornea. *Invest Ophthalmol Vis Sci.* 2020;61(6):37. <https://doi.org/10.1167/iovs.61.6.37>

PURPOSE. Autonomous molecular circadian clocks are present in the majority of mammalian tissues. These clocks are synchronized to phases appropriate for their physiologic role by internal systemic cues, external environmental cues, or both. The circadian clocks of the in vivo mouse cornea synchronize to the phase of the brain's master clock primarily through systemic cues, but ex vivo corneal clocks entrain to environmental light cycles. We evaluated the underlying mechanisms of this difference.

METHODS. Molecular circadian clocks of mouse corneas were evaluated in vivo and ex vivo for response to environmental light. The presence of opsins and effect of genetic deletion of opsins were evaluated for influence on circadian photoreponses. *Opn5*-expressing cells were identified using *Opn5^{Cre};Ai14* mice and RT-PCR, and they were characterized using immunocytochemistry.

RESULTS. Molecular circadian clocks of the cornea remain in phase with behavioral circadian locomotor rhythms in vivo but are photoentrainable in tissue culture. After full-thickness incision or epithelial debridement, expression of the opsin photopigment *Opn5* is induced in the cornea in a subset of preexisting epithelial cells adjacent to the wound site. This induction coincides with conferral of direct, short-wavelength light sensitivity to the circadian clocks throughout the cornea.

CONCLUSIONS. Corneal circadian rhythms become photosensitive after wounding. *Opn5* gene function (but not *Opn3* or *Opn4* function) is necessary for induced photosensitivity. These results demonstrate that opsin-dependent direct light sensitivity can be facultatively induced in the murine cornea.

Keywords: *opn5*, cornea, neuropsin, circadian rhythm, corneal wound

Most tissues in mammals exhibit autonomous molecular circadian clocks that adopt specific phases within the entrained animal, typically by responding to timing cues from the brain's master clock, the suprachiasmatic nuclei (SCN).¹ The phase of the SCN is synchronized to the 24-hour solar cycle through light information relayed by *Opn4*-expressing retinal ganglion cells.² Loss of the SCN causes behavioral sleep-wake and hormone rhythms to become arrhythmic.^{3,4} While peripheral clocks may remain oscillatory in SCN-lesioned animals, the phases of these clocks scatter within the same organism.⁵ The full mechanisms by which the SCN maintains synchrony of specific peripheral clocks is an area of active inquiry, but it appears that most individual tissue clocks synchronize their rhythms to the SCN using some combination of systemic circulating factors (particularly glucocorticoids⁶), neural input (particularly through the autonomic nervous system⁷), or oscillating physiologic parameters (such as body temperature^{8,9}).

Two tissues—retina and skin—appear to be exceptions to this mechanism. Circadian clocks within the retina and exposed skin of mice are directly photoentrained (synchronized by photons) to environmental light cycles and can do so regardless of the locomotor activity phase of the animal.¹⁰⁻¹² Both of these phenomena require the function of the opsin protein OPN5 (neuropsin).^{11,12} Interestingly, the retina uses a combination of classical (rhodopsin) and novel (*Opn5*) opsins for local clock entrainment.^{11,13} In mammals, OPN5 is one of the “noncanonical” opsin photoreceptors, along with OPN3 and OPN4, which mediate the effects of light outside of classical visual pathways.² OPN5 is maximally sensitive to short-wavelength light (~380 nm, λ_{max})^{14,15} and in mice contributes to circadian photoentrainment of individual tissues,¹¹ photoentrainment of locomotor rhythms,¹⁶ and development of retinal vasculature.¹⁷ In birds, OPN5 functions as a photoreceptor in both the retina and hypothalamic areas.¹⁸⁻²⁰

The murine cornea expresses robust circadian rhythms of clock gene expression in the majority of cells throughout the epithelium and endothelium both in vivo and ex vivo.^{5,21,22} Synchronization of corneal phase to the light-dark cycle appears to be influenced by both melatonin and glucocorticoids,^{21,23,24} suggesting circulating systemic cues set the phase of this tissue from the master clock. However, murine cornea has also been shown to express OPN4 and OPN5.^{11,25,26} OPN4 expression in the cornea appears to occur in neural tissue and contribute to light-induced photosensitivity (allodynia).^{25,27} Murine cornea has also been shown to be directly photoentrainable ex vivo via an *Opn5*-dependent mechanism.¹¹ The current study was designed to determine whether murine cornea primarily uses systemic humoral or local photic mechanisms for its entrainment and synchronization to the light-dark cycle. We also wished to assess the contributions of the noncanonical opsins in corneal photoreception.

METHODS

Animals

All animal experiments were carried out according to Institutional Animal Care and Use Committee guidelines at University of Washington, Seattle, WA, and adhere to the ARVO statement for the Use of Animals in Ophthalmic and Vision Research. *Opn5^{Cre};Ai14* was created as described in Nguyen et al.¹⁷ *Opn5^{-/-}* and *Opn3^{-/-}* mice were as described in Buhr et al.¹¹ *Opn4^{-/-}* mice were described in Panda et al.²⁸ *Pde6b^{rd1/rd1}* on a C57BL6/J background was purchased from Jackson Laboratories, strain: 004766. *Per2^{Luciferase}* mice were as initially described in Yoo et al.⁵ Male and female mice between 1 month and 1 year of age were used for all experiments.

Animal Behavior and Behavioral Desynchrony

Opn4^{-/-}; *Pde6b^{rd1/rd1}* mice lack functional rods, cones, and melanopsin function and behaviorally free-run rather than entrain to light-dark cycles. By maintaining these animals in light-dark 12:12 (LD 12:12) cycles, desynchrony between the external light-dark cycle and the SCN-driven phase of behavior will occur in all animals. By assessing the phase of the circadian clock in specific tissues via measurement of clock-gene expression, it can be determined whether a given tissue remains synchronized to the behavioral (SCN) clock or directly to the light-dark cycle. *Opn4^{-/-}*; *Pde6b^{rd1/rd1}* mice were singly housed in cages that contained running wheels, and wheel revolutions were monitored by a microswitch connected to a computer. Behavioral traces were collected and analyzed using ClockLab software (Actimetrics, Evanston, IL, USA). Behavioral onsets were monitored in free-running mice using a fit-line to the average onsets over at least 7 days. After at least 21 days in a 12-hour light/12-hour dark cycle, behavior was observed for days at which mice were beginning behavioral onset coincident with lights-on or (in a separate group of mice) lights-off. On these days, mice were euthanized with CO₂ asphyxiation and their corneas were rapidly dissected in cold Hanks' balanced salt solution (HBSS) in dim red light. Five mice were sacrificed for each group at each time point. Light in the light-dark cycle consisted of 3 LEDs of 415 nm (4.2×10^{14} photons cm⁻² s⁻¹), 475 nm (7.2×10^{14} photons cm⁻² s⁻¹), and 530 nm (4×10^{13} photons cm⁻² s⁻¹).

RNA Isolation and RT-PCR

For all RNA isolation, tissues were homogenized in TriReagent (Ambion, Thermo Fisher) according to the manufacturer's protocol. RNA was reverse transcribed into cDNA using the High Capacity RNA to cDNA kit (Applied Biosystems, Thermo Fisher, USA). Quantitative $\Delta\Delta C_t$ PCR was carried out on an ABI 7500Fast machine (Applied Biosystems) using Power Up SYBR Green master mix (Applied Biosystems, Thermo Fisher, USA). The rhythmic quality of the data was analyzed using CircWave 1.4 (www.euclock.org, Netherlands).²⁹ Briefly, a sinusoid fit to the data is compared to a horizontal line at the mean of the data. Linear harmonic regression is used to generate probability of rhythmic variation from the mean. All transcripts were normalized to β -actin using the primers shown in Table 1.

Per2: Luciferase Reporter Photoentrainment and Phase Shifts

Per2^{Luciferase} mice were euthanized by CO₂ asphyxiation, and their eyes were quickly removed and transferred to ice-cold HBSS (Gibco, USA). In dim white light, corneas were removed using two scalpel blades and cultured on cell culture inserts (PICMORG50; Millipore, USA). They were incubated in sealed petri dishes in DMEM (Cellgro; USA) containing B-27 serum-free supplement (Life Technologies, USA), 0.1 mM D-Luciferin potassium salt (Biosynth; USA), 352.5 μ g/mL sodium bicarbonate, 10 mM HEPES, and 25 U/mL penicillin, 25 μ g streptomycin (Life Technologies). Dishes were cultured at 36°C in a Lumicycle photomultiplier tube luminometer machine (Actimetrics, USA) contained within an air-jacketed incubator. Because the phase of cornea cultures is influenced by the time of dissection,³⁰ all experiments here used sealed cultures throughout the experiment, and the phase of the fellow cultured cornea was used as a phase control for treatment groups. For light pulses, one cornea culture was transferred in an insulated shuttle box to another incubator equipped with an LED array for 90 minutes and exposed to light at the indicated wavelength/intensity. For each light pulsed cornea, the fellow cornea was transferred to the LED incubator at the same time in a separate shuttle box covered with aluminum foil. Phase shifts were calculated as the phase difference between the fellow corneas using Lumicycle Analysis software (Actimetrics). For ex vivo photoentrainment, cornea pairs (right and left eye) from individual mice were maintained as sealed organotypic tissue cultures and exposed to oppositely phased LD 9:15 light-dark cycles (2×10^{14} photons cm⁻² s⁻¹, 415 nm) for 4 days after dissection (this light cycle has previously been shown to be optimal for demonstrating ex vivo entrainment of retina,³¹ cornea,¹¹ and skin¹²). The dishes were then transferred to constant darkness, and the phases of the *Per2^{Luciferase}* luminescence rhythms were measured using Lumicycle Analysis software (Actimetrics).

Relaxing incisions were made for most experiments so that the cornea would lie flat on the cell culture insert. Images were made of tdTomato fluorescence from *Opn5^{Cre/+};Ai14* corneas using a fluorescence microscope. For time course experiments, an individual *Opn5^{Cre/+};Ai14* cornea was maintained at 36°C on the microscope stage using a stage top incubator (Bioscience Tools, USA). For algerbrush experiments, an algerbrush with a 0.5-mm burr (Strong Vision Technology, Jackson, MI, USA) was used to deepithelialize a region of the cornea of a euthanized mouse

TABLE 1. Primers used in RT-PCR

Transcript (Amplicon Size)	Forward	Reverse
<i>Opn5</i> (218 bp)	5' AGCTTTTGGGAAGGCCAGAC	5' CAGCACAGCAGAAGACTTC
<i>Opn4</i> (180 bp)	5' TCTGTTAGCCCCACGACATC	5' TGAACATGTTTGCTGGTGTCC
<i>Opn3</i> (227 bp)	5' CTGTTCCGGAGTCACCTTCAC	5' GTATGTCTAGGATGTACCTGTTC
<i>Hprt1</i> (142 bp)	5' TCAGTCAACGGGGGACATAAA	5' GGCTGTACTGCTTAACCAG
<i>Gapdh</i> (75 bp)	5' CAAGGAGTAAGAAACCCTGGACC	5' CGAGTTGGGATAGGGCCTCT
<i>β-actin</i> (188 bp)	5' AGGTGACAGCATTGCTTCTG	5' GCTGCCTCAACACCTCAAC
<i>Per2</i> (216 bp)	5' CCAACACAGACAGACAGATC	5' TCTCGCAGTAAACACGCCT
<i>Per1</i> (91 bp)	5' CCCAGCTTACCTGCAGAAG	5' ATGGTCGAAAGGAGCCTCT
<i>Bmal1</i> (200 bp)	5' GACATTTCTCAACCATCAGCG	5' GCATTCTTGATCCTTCTGGT
<i>Dbp</i> (118 bp)	5' CGAAGAACGTCATGATGCAG	5' GGTTCCTCAACATGCTAAGA

TABLE 2. Antibodies used in Immunofluorescence

Antibodies	Source	Concentration	Catalog number
Cytokeratin 12 (KRT12)	Proteintech	1:200	24789-1-AP
Cytokeratin 14	Proteintech	1:100	10143-1-AP
Pax6	Proteintech	1:200	12323-1-AP
Cytokeratin 15	Proteintech	1:200	10137-1-AP
Anti-mouse TCR γ/δ antibody (GL3)	Biolegend	1:500	118101
CD11c monoclonal antibody (N418)	invitrogen	1:200	14-0114-81
CD11b monoclonal antibody (M1/70)	invitrogen	1:200	14-0112-82
APC anti-mouse CD45 (30-F11)	Biolegend	1:200	103111
Keratocan anti-mouse	gift	1:200	32

prior to the eye being removed. For these corneas, small relaxation incisions were made away from the deepithelialization region.

Immunofluorescence

Whole corneas were fixed in 4% Paraformaldehyde (PFA)/PBS at room temperature (RT) for 15 minutes followed by permeabilization with Triton X-100 1% for 30 minutes. After this, corneas were incubated for 1 hour in blocking buffer (2.5% normal goat serum, 2.5% normal donkey serum, 2% gelatin, 1% BSA, 0.2% Triton X-100). Corneas were incubated in different primary antibodies (Table 2) overnight at 4°C. After incubation, samples were rinsed in PBS, incubated with secondary antibody goat anti-rabbit–Alexa 633 (Invitrogen, USA) for 1 hour at RT, and mounted with ProLong Gold Antifade Mountant with 4', 6-diamidino-2-phenylindole (DAPI) (Invitrogen).

For EdU incorporation, corneas were incubated as described above. EdU was added to the media for a 20- μ M final concentration. Corneas were collected at 24 to 48 hours. To inhibit cell division, cytosine arabinoside (ARA-C; Millipore Sigma, USA) was added in the media at the beginning of the experiments where noted. EdU staining was performed following the manufacturer's protocol using the Click-iT EdU Alexa Fluor 647 imaging kit (Invitrogen). Immunofluorescent images were analyzed using a Leica (Germany) DM6000 microscope with a Leica SP8 confocal system and processed with FIJI/ImageJ (National Institutes of Health, Bethesda, MD, USA).

RESULTS

Corneal Circadian Clocks Directly Photoentrain Ex Vivo but Not In Vivo

To assess if the circadian clock genes of corneas synchronize to light-dark cycles in vivo, we performed analyses

of clock gene transcript abundance in corneas of behaviorally desynchronized mice (see Methods). We have previously used this experimental design to demonstrate direct photoentrainment of murine retina³¹ and skin¹² clocks to light-dark cues, while other tissues such as pituitary and liver remain tied to behavioral phase. *Opn4*^{-/-}; *Pde6b*^{rd1/rd1} mice were exposed to 12-hour light/12-hour dark cycles, and the onset of their running wheel activity was used as a measure of the phase of their internal, SCN-driven phase (Fig. 1A). After at least 3 weeks, we monitored their activity for times at which one cohort of mice began activity at the dark-to-light transition and another began activity at the light-to-dark transition (as has been described previously¹²). On the day at which the behavioral onsets of the two groups of mice were at opposite phases relative to the light cycle, tissues were collected at four time points across the day. We analyzed the transcript abundance of the clock genes *Per2*, *Per1*, *Bmal1*, and *Dbp* relative to *β-actin* using RT-PCR from the corneas of each cohort. Unlike previous results from retina and skin,^{12,31} analyses of the phases in the rhythmic expression of clock genes in the cornea using linear harmonic regression sine waves (fit using CircWave 1.4³³) revealed an alignment with behavioral phase, not the light-dark cycle (Fig. 1B). This indicates that the circadian clocks of the healthy cornea are not directly synchronized by light in vivo.

However, these data are not consistent with our earlier observation that the *Per2*^{Luciferase} rhythms of wild-type corneas can be photoentrained ex vivo,¹¹ and it is possible that the mutation of *Opn4* or *Pde6b* could impair the cornea's photosensitivity. We next tested ex vivo photoentrainment for 4 days (see Methods) in corneas of wild-type; *Per2*^{Luciferase} or *Opn4*^{-/-}; *Pde6b*^{rd1/rd1}; *Per2*^{Luciferase} mice (Fig. 1C). Upon transfer to constant darkness, the phases of the *Per2*^{Luciferase} luminescence rhythms of cornea pairs from the same animals displayed opposite phases reflecting the phase of the previous light-dark cycle (Fig. 1C), confirming ex vivo photoentrainment of corneal tissue and demon-

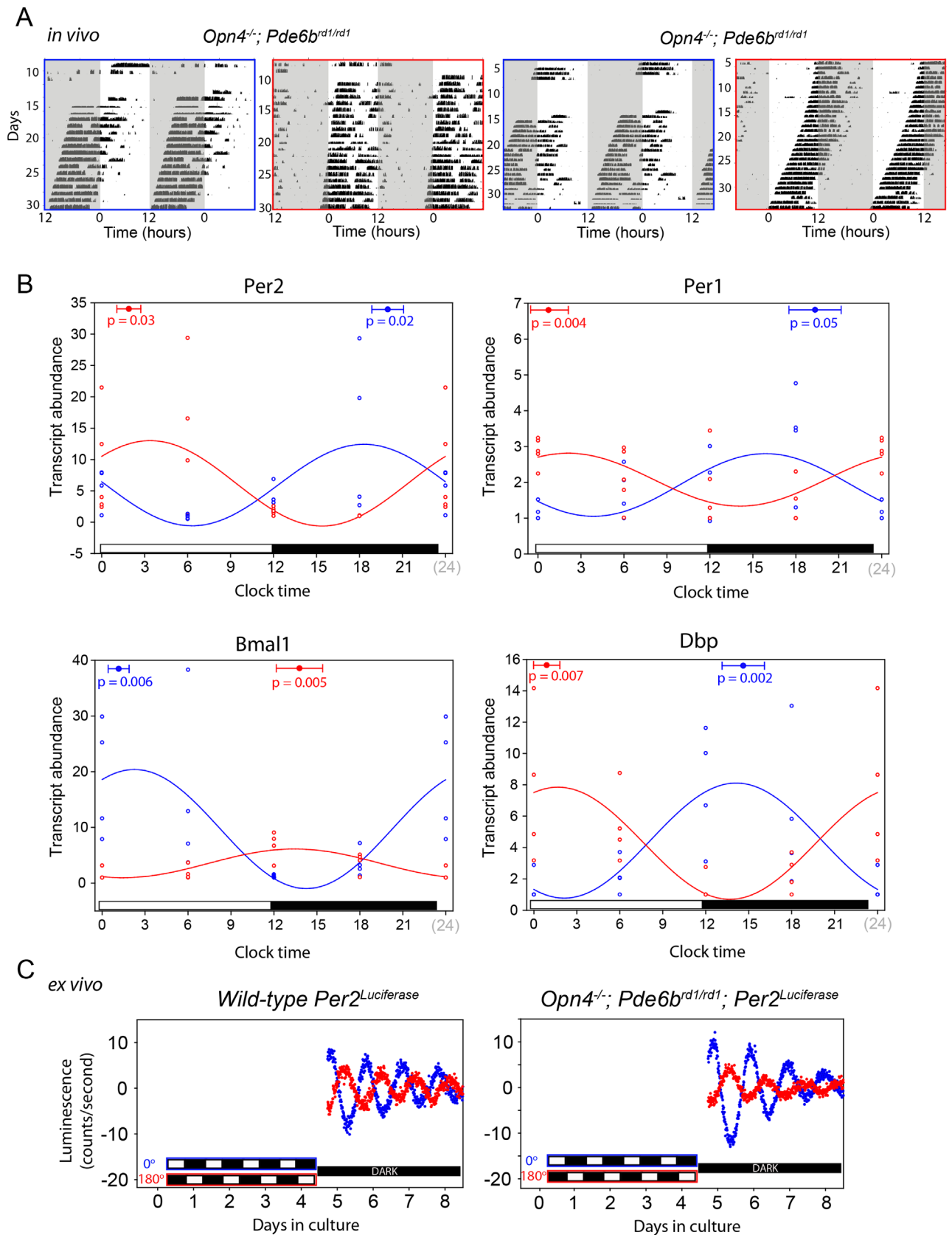


FIGURE 1. Cornea circadian clocks photoentrain ex vivo but not in vivo. (A) Wheel-running activity of *Opn4^{-/-}; Pde6b^{rd1/rd1}; Per2^{Luciferase}* mice in light (*ubite*)/dark (*gray*) cycles. Tissue was collected when the behavioral onset coincided with either lights-off (*blue frame*) or lights-on (*red frame*). (B) RT-PCR of the indicated transcripts using the $\Delta\Delta Ct$ method relative to β -actin transcript. *Open circles* represent values from individual corneas from either in-phase/lights-off (*blue*) or out-of-phase/lights-on (*red*) mice. *n* = 5 for each time point, for

each animal group. Curves represent fit sine waves using CircWav software. The solid points with error bars represent the center of gravity \pm SEM and the P value of the fit rhythm compared to the horizontal average of the data. (C) *Per2^{Luciferase}* bioluminescence rhythms after 4 days of oppositely phased light-dark cycles. Red and blue traces represent cultures of individual corneas from the same mouse from either a wild-type; *Per2^{Luciferase}* (left) or *Opn4^{-/-}*; *Pde6b^{rd1/rd1}*; *Per2^{Luciferase}* (right).

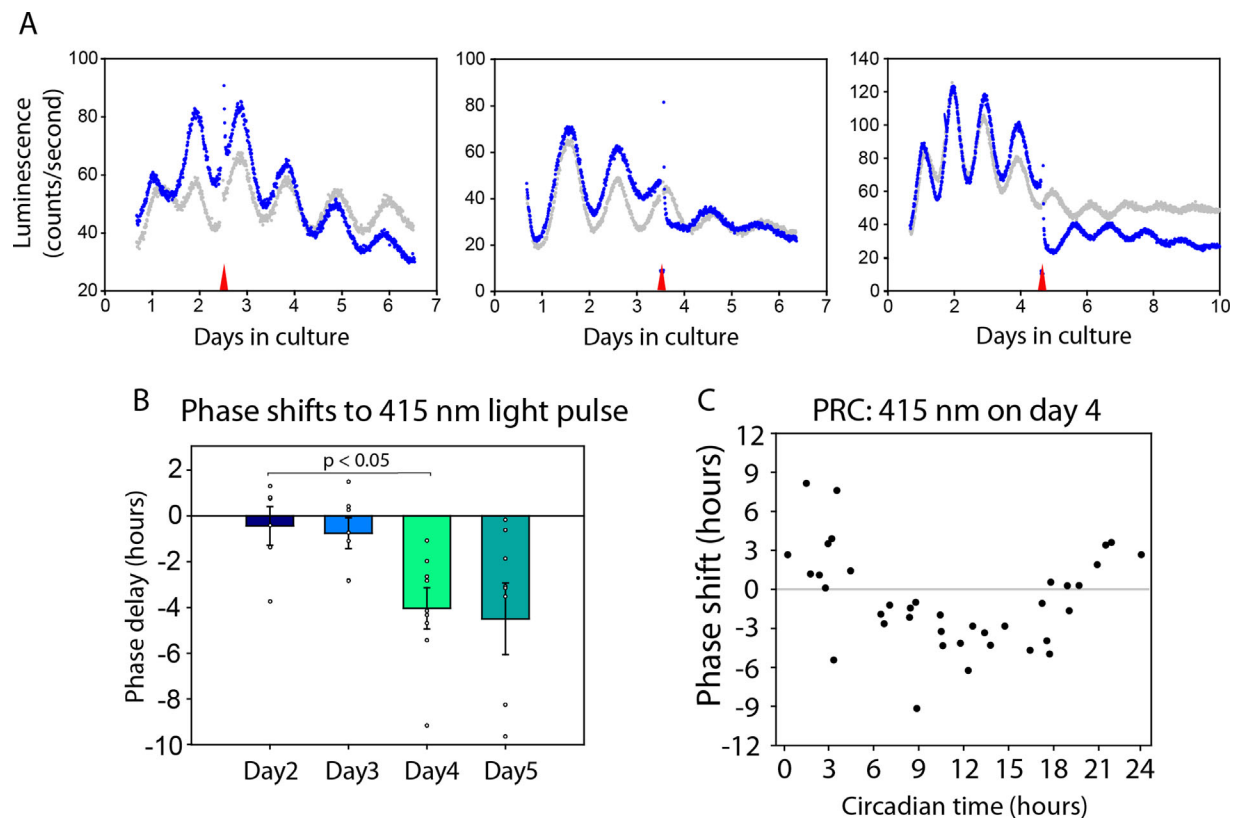


FIGURE 2. Photic responses of circadian clocks in cultured corneas emerge over time in culture. (A) *Per2^{Luciferase}* rhythms from corneas receiving a 90-minute 415-nm light pulse (blue) or a dark pulse (gray) at the time indicated by a red arrow. (B) Phase delays of light-treated corneas compared to dark-handled controls of the same animals. Bars represent mean \pm SEM. $P < 0.05$ in ANOVA with Tukey post hoc analysis where noted. $n = 8$ for each group. (C) Phase response curve of cultured corneas receiving a 90-minute 2×10^{14} photons $\text{cm}^{-2} \text{s}^{-1}$ pulse of 415-nm light at the indicated circadian phase. $n = 38$.

strating that *Opn4* and *Pde6b* are not required for ex vivo photoentrainment of mouse corneas.

***Opn5*-Dependent Photic Responses of the Circadian System in Cornea Emerge Ex Vivo**

To further characterize the light response of cultured corneas, we administered 90-minute pulses of 2×10^{14} photons $\text{cm}^{-2} \text{s}^{-1}$ 415-nm light to corneas during early subjective night and measured resulting circadian phase changes. After 1 day of culture, there was no shift in the *Per2^{Luciferase}* luminescence rhythms of a light-treated cornea compared to a dark-treated control from the fellow eye (Fig. 2A). However, after approximately 3 days of culture, large phase delays were observed in light-pulsed corneas (Fig. 2B). When similar light pulses were administered at phases across the circadian cycle on the fourth day of culture, phase delays and advances were observed at specific times of day characteristic of a “type 1” phase response curve (PRC) (Fig. 2C).³⁴

In previous work, we observed that the photoentrainment of circadian clocks in the cornea was dependent on the expression of *Opn5*.¹¹ To test whether the spectral sensitivity of the photic phase shifting in corneas fit with this observation, we exposed corneas to 2×10^{14} photons $\text{cm}^{-2} \text{s}^{-1}$ monochromatic light after 4 days in culture at a phase predicted to elicit a large phase delay (based on the PRC of Fig. 2C). Light of 400 nm and 415 nm produced large phase shifts, whereas 530-nm light did not shift the phase of the cornea clocks (Fig. 3A). This is consistent with the function of a short wavelength-sensitive photoreceptor. To test the involvement of noncanonical opsin expression, we administered 415-nm light pulses to corneas from *Opn3^{-/-}*, *Opn4^{+/-}*, *Opn5^{+/-}*, and *Opn4^{+/-}*; *Opn5^{+/-}* mice on the fourth day in culture. Wild-type, *Opn3^{-/-}*, and *Opn4^{+/-}* corneas responded with similar phase shifts, which were significantly different from dark-handled controls (Fig. 3B, $P < 0.05$ ANOVA, Tukey post hoc). The circadian phase of the *Opn5^{+/-}* and *Opn4^{+/-}*; *Opn5^{+/-}* corneas did not respond to light pulses, confirming the necessity of *Opn5* in the corneal light response (Fig. 3B).

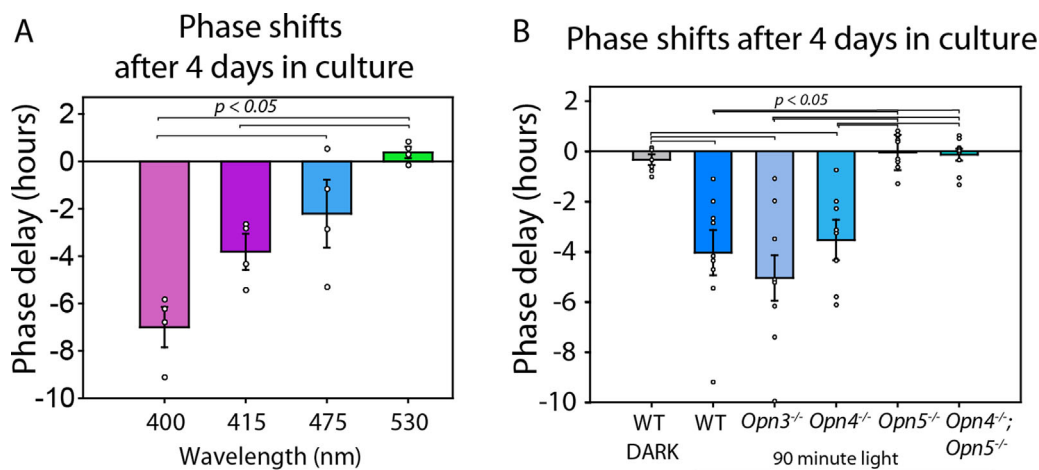


FIGURE 3. Light response of the circadian clock requires OPN5. (A) Phase delays of cultured corneas after 4 days of culture receiving a 90-minute 2×10^{14} photons $\text{cm}^{-2} \text{s}^{-1}$ light pulse of the indicated wavelength between circadian time (CT) 11 to 13. $n = 4$ for each group. (B) Phase delays of cultured corneas after 4 days of culture receiving a 90-minute 2×10^{14} photons $\text{cm}^{-2} \text{s}^{-1}$ pulse of 415-nm light at CT 11 to 13 from mice of the indicated genotypes. Bars represent mean \pm SEM. $P < 0.05$ in ANOVA with Tukey post hoc analysis. $n = 8$ in each group.

Induction of *Opn5* Gene Expression in Cultured Cornea

From these data, it appeared that direct, *Opn5*-dependent shortwave light sensitivity of the cornea developed following explantation. One possibility for this would be that *Opn5* expression is upregulated following dissection. We assessed the level of opsin transcript relative to β -actin in corneas maintained in organotypic culture. A large increase of *Opn5* transcript expression was observed after 2 days in culture (Fig. 4A). A smaller but significant increase in *Opn4* transcript was also detected relative to the fresh cornea (day 0). Transcript levels were variable but not significantly increased for *Opn3* (Fig. 4A). Unfortunately, no validated antibodies to OPN5 protein have been described.¹¹ In order to better characterize the *Opn5* induction in a single cornea over time, an *Opn5*^{Cre}; *Ai14* (tdTomato) reporter¹⁷ was used to observe *Opn5*^{Cre} induction over multiple days ex vivo (3-hour resolution for 48 hours; see Supplementary Video). We noted two populations of *Ai14*-positive cells. A sparse, stationary group of cells in the corneal stroma is present at time of dissection; we refer to these cells as “type 0” as they are present at timepoint 0 relative to explantation. In contrast, we noted marked induction of *Ai14* expression in the epithelium (type 1 cells) starting at about 9 to 12 hours postdissection. These cells appear to be highly motile (see Supplementary Video). The type 1 cells display a morphology typical of epithelial cells with rounded, flat cell bodies, while the type 0 cells have much larger cell bodies and outreaching dendritic processes similar to dendritic cells (Figs. 4D, 4E).

It is possible that the type 1 cells are induced in response to corneal wounding. To explore this using a widely used model of corneal injury, we performed a deep-epithelialization of the central cornea using an algerbrush immediately following euthanasia of *Opn5*^{Cre}; *Ai14* mice. The corneas were then maintained ex vivo and imaged for tdTomato expression. We observed a pronounced induction of type 1 cells in the debridement zone of the wound compared to nonwounded areas (Supplementary Fig. S1A). The wounded area showed an increase of 14.4 ± 4.3

tdTomato-positive cells/ mm^2 by 24 hours after debridement, compared with 4.6 ± 0.8 cells/ mm^2 in the same area of nonwounded cornea (paired *t*-test, $P = 0.017$, $n = 5$; Supplementary Fig. S1B).

We sought to determine if the type 1 cells were nascent cells rapidly dividing along wound sites or if these were preexisting cells being triggered to express the opsin. Immediately after dissection, corneas from *Opn5*^{Cre}; *Ai14* mice were incubated with EdU (Click-iT EdU; Thermo Fisher), which is incorporated into cells undergoing the DNA synthesis phase of cell division. Proliferating cells incorporating the modified uridine were then imaged by detection of a fluorescent tag (Alexa Fluor, 647 nm). Many recently divided cells were readily identified within 12 hours of culture, and by 24 hours, the corneal epithelium was populated by $1.2 \times 10^4 \pm 641$ cells/ mm^2 labeled with EdU (Fig. 5A). When we compared the tdTomato expression from the *Ai14* transgene with the EdU-labeled cells, there was little coexpression. Only $10.1\% \pm 3.1\%$ ($n = 6$) of the tdTomato-positive type 1 cells also contained EdU by 24 hours (Figs. 5B, 5C). Thus, it is likely that the majority of the cells that induced *Opn5* were cells already resident in the cornea at the time of dissection or injury. Similarly, type 1 cells induced by an epithelial debridement did not incorporate EdU (Supplementary Fig. S2C).

To further validate this finding, we exposed cultured corneas to ARA-C to inhibit synthesis of DNA and block cell division.³⁵ A total of 50 μM Ara-C ex vivo was sufficient to block proliferating cells at 24 hours as measured by EdU (Fig. 5D). The same treatment had no discernible impact on the induction of type 1 *Opn5*^{Cre}; *Ai14* expressing cells (Fig. 5E). ARA-C treatment also had no effect on the period or amplitude of the circadian rhythm as measured by *Per2*^{Luciferase} activity in cultured corneas, indicating that the treatment was not toxic (Supplementary Fig. S2).

Identity of *Opn5*-Expressing Corneal Cells

The type 1 corneal cells with induced *Opn5*^{Cre}; *Ai14* are found throughout the epithelium, from basal to suprabasal

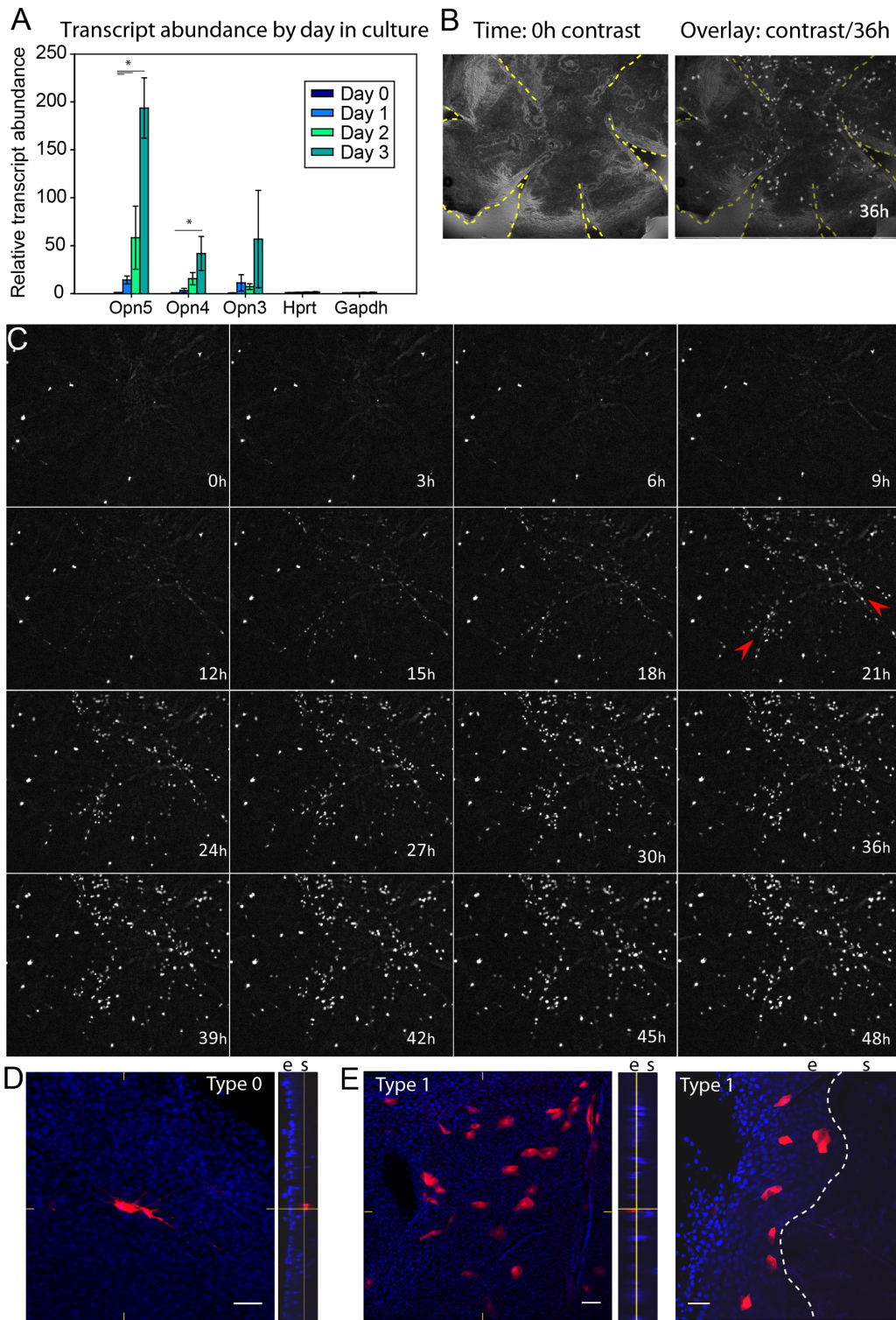


FIGURE 4. Opn5 induction after culture of cornea. **(A)** Relative abundance of the indicated transcript compared to β -actin using the $\Delta\Delta Ct$ quantitative PCR method in fresh or cultured mouse corneas. Bars represent mean \pm SEM. $n = 4$. **(B)** White-light contrast image of cornea in **C** at time 0. Yellow dashed line shows sites of relaxation incisions. **(C)** Fluorescence images of an *Opn5Cre; Ai14* cornea taken at the indicated time postdissection. Red arrows in 21-hour image highlight relaxation incisions. **(D)** Fluorescence images of *Opn5Cre; Ai14* (red) expression and DAPI-stained nuclei (blue) of a type 0 cell. Scale bar: 50 μ m. Right panel shows Z projection of image at left. e, epithelium; s, stroma. **(E)** Fluorescence images of *Opn5Cre; Ai14* (red) expression and DAPI-stained nuclei (blue) of type 1 cells in en face (left) or diagonal-cut (right) corneas. Scale bar: 50 μ m.

layers, and show typical morphology of epithelial cells (Fig. 4E). These cells were colabeled with antibodies for K14,

K12,^{36,37} and PAX6,^{38,39} confirming their identity as epithelial cells (Figs. 6A–C). Furthermore, we did not observe any

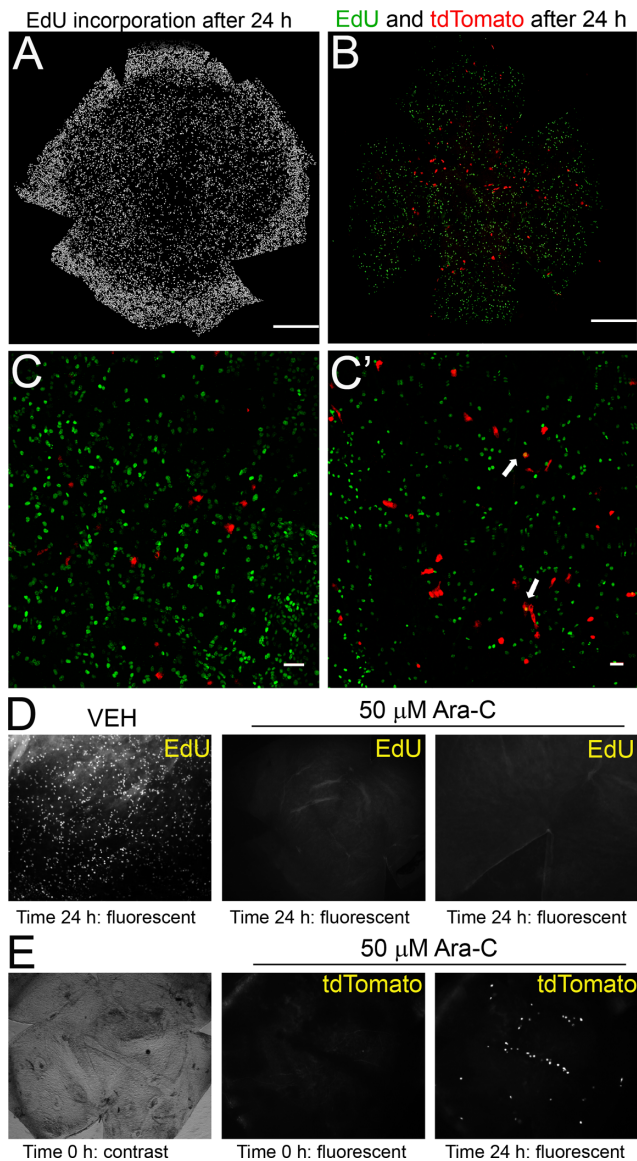


FIGURE 5. Cells with induced *Opn5* are resident cells. (A) Fluorescence image of EdU incorporation in a whole-mounted cornea after 24 hours in culture. Scale bar: 200 μ m. (B) EdU-incorporated cells (green) and *Opn5*^{Cre}; *Ai14* tdTomato cells (red) after 24 hours in culture. Scale bar: 200 μ m. (C) Same as B but with higher magnification. Scale bars: 50 μ m. Arrows point to two colabeled cells. (D) EdU-incorporated cells in vehicle (left) and two examples of 50 μ M ARA-C-treated corneas as whole mounts after 24 hours in culture. (E) Brightfield illumination (left) and fluorescence image (center) of an *Opn5*^{Cre}; *Ai14* cornea immediately after dissection into 50 μ M ARA-C. The same cornea showing tdTomato-positive cells after 24 hours.

colabeling of the *Opn5*^{Cre}; *Ai14* cells with K15, distinguishing these cells from limbal epithelial cells (Fig. 6D).⁴⁰ Finally, because of their induction after wounding, morphology, and lack of proliferative markers, we also considered that they bear a resemblance to corneal $\gamma\delta$ T cells.^{41,42} However, we did not detect colabeling with TCR δ GL3 or CD45 and tdTomato (Figs. 6E, 6F). Thus, the damage-induced *Opn5*-expressing type 1 cells appear to be central corneal K14+ epithelial cells.

The identity of the larger type 0 cells is still undetermined. Because of the morphology, location in the upper stroma/basal epithelium, and lack of proliferative markers, we considered the type 0 cells may be resident dendritic cells or macrophages.^{43,44} However, these cells were not colabeled with CD11c (dendritic cells) or CD11b (macrophages) (Supplementary Fig. S3A). Rather, we observed colabeling with a keratocan antibody, suggesting that these cells are a subset of keratocytes.³² It should be noted that the *Opn5*^{Cre}; *Ai14* reporter system is a lineage-marking *loxP*-based reporter. This means that cells expressing tdTomato at the start of an experiment may be expressing *Opn5* actively or may be lineage-derived from *Opn5*-expressing cells. While the type 1 epithelial cells were induced during each experiment (indicating active *Opn5*-expression), the type 0 cells were present throughout the experiments. Also, because the type 0 cells are present at times when the cornea circadian clocks are not light responsive (Fig. 2), it is unlikely that they are responsible for the phenomena.

DISCUSSION

We have demonstrated that in vivo, circadian phase entrainment of corneal rhythmicity is driven by systemic cues linked to the phase of SCN and behavior rather than the direct light-dark cycle. This result corroborates earlier findings from corneas of *Opn4*::TeNT mice.⁴⁵ However, once the cornea has been explanted, it becomes photoentrainable and exhibits phase shifts to light. This induced photosensitivity is maximally sensitive to short visible wavelengths and requires *Opn5* (but not *Opn4* or *Opn3*). Photosensitivity corresponds to induction of *Opn5* expression, which appears to localize in a preexisting, small subset of corneal epithelial cells concentrated in areas of injury. Taken together, these results demonstrate that corneal injury results in induction of local photosensitivity in the corneal epithelium via an *Opn5*-dependent mechanism that is sufficient to permit direct circadian photoentrainment.

Opsin-mediated extraretinal photoreception has long been known in fish,^{46,47} amphibians,^{48,49} reptiles,^{50,51} and birds.^{19,52} In brains of birds, pinopsin is expressed in the pineal gland and regulates melatonin synthesis,⁵³ and *Opn5* is expressed in the hypothalamus and regulates breeding based on seasonal changes in day length.^{19,20} Similarly, teleost fish express opsins in many tissues, and these tissues are photosensitive to prolonged light exposure.⁵⁴ Until recently, it was believed that in mammals, only the retina demonstrated opsin-mediated photosensitivity. The catalog of vertebrate tissues that have been found to express opsins has expanded dramatically in recent years.⁵⁵ Mice have been shown to express opsins in their skin,^{15,56} as well as in their brain (*Opn3* and *Opn5*),^{57,58} testis (*Opn5*),⁵⁷ adipose tissue (*Opn3*),⁵⁹ vascular smooth muscle,^{60,61} iris (*Opn4*),⁶² and ciliary body (*Opn5*).⁶³ Recent work has suggested a photosensitive role for *Opn3* in regulating metabolism in murine adipose tissue^{59,64} and has demonstrated that *Opn5* functions as a photopigment synchronizing circadian entrainment in skin in vivo.¹² Pulmonary arterial diameter has also recently been shown to be light sensitive and use an *Opn4*-dependent mechanism.⁶¹ In human tissue, it has been demonstrated that skin expresses *Opn1sw*, *Opn2*, *Opn3*, *Opn4*, and *Opn5*,^{65–67} suggesting that extraretinal, opsin-mediated photoreception may extend to humans as well.

Recent evidence suggests that the anterior segment of the eye, including the cornea, contains photoreceptors.^{62,63}

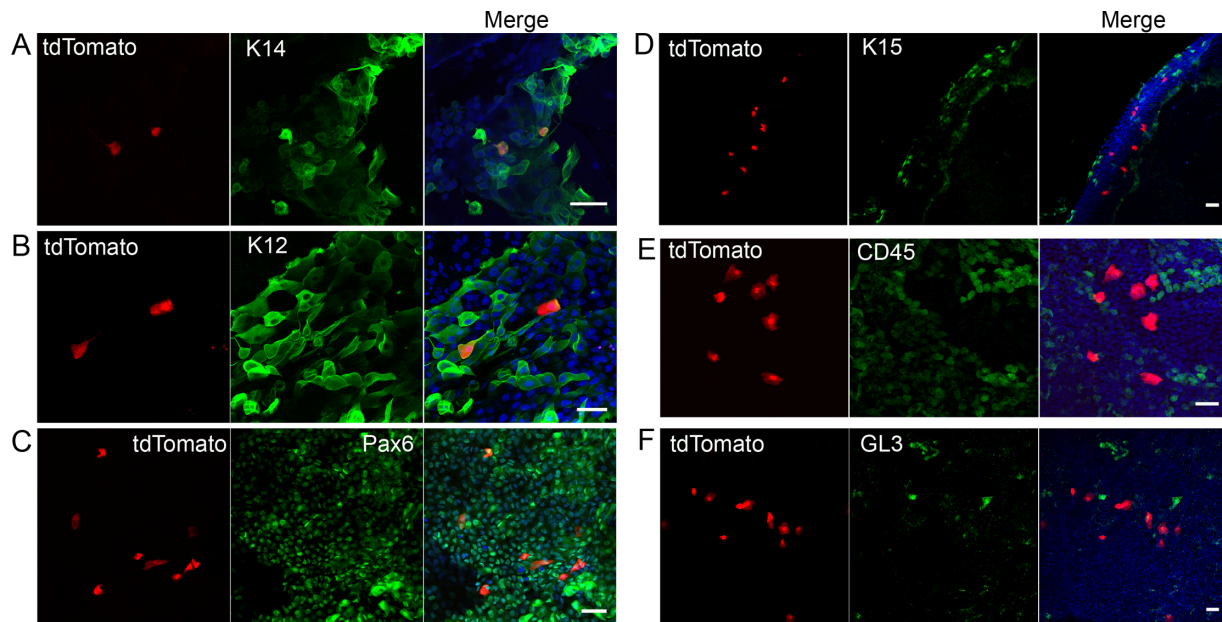


FIGURE 6. Cells with induced *Opn5* are epithelial cells. Fluorescent images of tdTomato from *Opn5Cre; Ai14* corneas (all left images) and (A) K14, (B) K12, (C) Pax6, (D) K15, (E) CD45, and (F) TCR GL3 (center images). Merged images at right also include nuclei (DAPI, blue). Scale bars: 50 μ m.

For example, the branch of the trigeminal nerve that innervates the cornea expresses *Opn4*.^{25,68} One potential role for this extra-retinal opsin is the photo-allodynia associated with corneal stress or migraine headache models, which may result from photic signals directly through these OPN4 cells in the trigeminal nerve.^{25,27} The current work now demonstrates a second opsin (*Opn5*) is expressed in cornea; however, *Opn5* appears to be expressed inducibly in corneal epithelial cells rather than in neurons, and it appears to be necessary and sufficient for induction of circadian photosensitivity. To our knowledge, the current study is the first to demonstrate inducible circadian photosensitivity in any tissue and the first to show rapid induction of opsin expression following injury.

The circadian clock and the time of wounding have an impact on the rate of healing in both skin and cornea.^{22,69,70} Light has been linked to enhanced dermal wound healing (or “photobiomodulation”); however, the necessary wavelengths, optimal procedures, and mechanisms of action remain unclear.⁷¹ In the cornea, the rate of mitosis in healing corneas is reduced in darkness compared to a light-dark cycle.²² One possible mechanism for altered healing in light-dark cycles could be enhanced synchronization of local circadian clocks allowing for a coordinated healing response. *Opn5* is induced along wound sites, which is consistent with a model of local clock synchronization influencing healing. Alternatively, it is possible that circadian entrainment is a by-product of other *Opn5*-mediated signals that are involved in wound healing. Future studies will assess the role of *Opn5* and light in corneal wound healing directly and whether any role is mediated by circadian clock-dependent mechanisms.

Acknowledgments

Supported by NIH R01 GM124246 to EDB, R01 EY026921 to RVG, NIH P30EY001730, the Latham Vision Research Innovation

Award, an unrestricted grant to the University of Washington Department of Ophthalmology from Research to Prevent Blindness, and the Mark J. Daily, MD Research Fund. This work was also supported by NIH grants R01 EY027077 and R01 EY027711 to RAL and by funds from the Goldman Chair of the Abrahamson Pediatric Eye Institute at Cincinnati Children’s Hospital Medical Center.

Disclosure: N.M. Díaz, None; R.A. Lang, None; R.N. Van Gelder, None; E.D. Buhr, None

References

- Mohawk JA, Green CB, Takahashi JS. Central and peripheral circadian clocks in mammals. *Annu Rev Neurosci.* 2012;35:445–462.
- Van Gelder RN, Buhr ED. Ocular photoreception for circadian rhythm entrainment in mammals. *Annu Rev Vis Sci.* 2016;2:153–169.
- Moore RY, Eichler VB. Loss of a circadian adrenal corticosterone rhythm following suprachiasmatic lesions in the rat. *Brain Res.* 1972;42:201–206.
- Stephan FK, Zucker I. Circadian rhythms in drinking behavior and locomotor activity of rats are eliminated by hypothalamic lesions. *Proc Natl Acad Sci USA.* 1972;69:1583–1586.
- Yoo SH, Yamazaki S, Lowrey PL, et al. PERIOD2::LUCIFERASE real-time reporting of circadian dynamics reveals persistent circadian oscillations in mouse peripheral tissues. *Proc Natl Acad Sci USA.* 2004;101:5339–5346.
- Balsalobre A, Brown SA, Marcacci L, et al. Resetting of circadian time in peripheral tissues by glucocorticoid signaling. *Science.* 2000;289:2344–2347.
- Buijs RM, Guzmán Ruiz MA, Méndez Hernández R, Rodríguez Cortés B. The suprachiasmatic nucleus; a responsive clock regulating homeostasis by daily changing the setpoints of physiological parameters. *Auton Neurosci.* 2019;218:43–50.

8. Brown SA, Zimbrunn G, Fleury-Olela F, Preitner N, Schibler U. Rhythms of mammalian body temperature can sustain peripheral circadian clocks. *Curr Biol*. 2002;12:1574–1583.
9. Buhr ED, Yoo SH, Takahashi JS. Temperature as a universal resetting cue for mammalian circadian oscillators. *Science*. 2010;330:379–385.
10. Tosini G, Menaker M. Circadian rhythms in cultured mammalian retina. *Science*. 1996;272:419–421.
11. Buhr ED, Yue WW, Ren X, et al. Neuropsin (OPN5)-mediated photoentrainment of local circadian oscillators in mammalian retina and cornea. *Proc Natl Acad Sci USA*. 2015;112:13093–13098.
12. Buhr ED, Vemaraju S, Diaz N, Lang RA, Van Gelder RN. Neuropsin (OPN5) mediates local light-dependent induction of circadian clock genes and circadian photoentrainment in exposed murine skin. *Curr Biol*. 2019;29:3478–3487.e3474.
13. Calligaro H, Coutanson C, Najjar RP, et al. Rods contribute to the light-induced phase shift of the retinal clock in mammals. *PLoS Biol*. 2019;17:e2006211.
14. Yamashita T, Ono K, Ohuchi H, et al. Evolution of mammalian Opn5 as a specialized UV-absorbing pigment by a single amino acid mutation. *J Biol Chem*. 2014;289:3991–4000.
15. Kojima D, Mori S, Torii M, Wada A, Morishita R, Fukada Y. UV-sensitive photoreceptor protein OPN5 in humans and mice. *PLoS One*. 2011;6:e26388.
16. Ota W, Nakane Y, Hattar S, Yoshimura T. Impaired circadian photoentrainment in Opn5-null mice. *iScience*. 2018;6:299–305.
17. Nguyen MT, Vemaraju S, Nayak G, et al. An opsin 5-dopamine pathway mediates light-dependent vascular development in the eye. *Nat Cell Biol*. 2019;21:420–429.
18. Rios MN, Marchese NA, Guido ME. Expression of non-visual opsins Opn3 and Opn5 in the developing inner retinal cells of birds: light-responses in Müller glial cells. *Front Cell Neurosci*. 2019;13:376.
19. Nakane Y, Ikegami K, Ono H, et al. A mammalian neural tissue opsin (Opn5) is a deep brain photoreceptor in birds. *Proc Natl Acad Sci USA*. 2010;107:15264–15268.
20. Nakane Y, Shimmura T, Abe H, Yoshimura T. Intrinsic photosensitivity of a deep brain photoreceptor. *Curr Biol*. 2014;24:R596–R597.
21. Baba K, Davidson AJ, Tosini G. Melatonin entrains PER2: LUC bioluminescence circadian rhythm in the mouse cornea. *Invest Ophthalmol Vis Sci*. 2015;56:4753–4758.
22. Xue Y, Liu P, Wang H, et al. Modulation of circadian rhythms affects corneal epithelium renewal and repair in mice. *Invest Ophthalmol Vis Sci*. 2017;58:1865–1874.
23. Pezuk P, Mohawk JA, Wang LA, Menaker M. Glucocorticoids as entraining signals for peripheral circadian oscillators. *Endocrinology*. 2012;153:4775–4783.
24. Cardoso SS, Sowell JG, Goodrum PJ, Fuste G. Effect of dexamethasone upon circadian mitotic rhythm in rat cornea. *Proc Soc Exp Biol Med*. 1972;140:1235–1239.
25. Matynia A, Nguyen E, Sun X, et al. Peripheral sensory neurons expressing melanopsin respond to light. *Front Neural Circuits*. 2016;10:60.
26. Delwig A, Chaney SY, Bertke AS, et al. Melanopsin expression in the cornea. *Vis Neurosci*. 2018;35:E004.
27. Marek V, Reboussin E, Dégardin-Chicaud J, et al. Implication of melanopsin and trigeminal neural pathways in blue light photosensitivity. *Front Neurosci*. 2019;13:497.
28. Panda S, Sato TK, Castrucci AM, et al. Melanopsin (Opn4) requirement for normal light-induced circadian phase shifting. *Science*. 2002;298:2213–2216.
29. Oster H, Damerow S, Hut RA, Eichele G. Transcriptional profiling in the adrenal gland reveals circadian regulation of hormone biosynthesis genes and nucleosome assembly genes. *J Biol Rhythms*. 2006;21:350–361.
30. Evans JA, Suen TC, Callif BL, et al. Shell neurons of the master circadian clock coordinate the phase of tissue clocks throughout the brain and body. *BMC Biol*. 2015;13:43.
31. Buhr ED, Van Gelder RN. Local photic entrainment of the retinal circadian oscillator in the absence of rods, cones, and melanopsin. *Proc Natl Acad Sci USA*. 2014;111:8625–8630.
32. Liu CY, Birk DE, Hassell JR, Kane B, Kao WW. Keratan-deficient mice display alterations in corneal structure. *J Biol Chem*. 2003;278:21672–21677.
33. Husse J, Leliavski A, Tsang AH, Oster H, Eichele G. The light-dark cycle controls peripheral rhythmicity in mice with a genetically ablated suprachiasmatic nucleus clock. *FASEB J*. 2014;28:4950–4960.
34. Winfree AT. Integrated view of resetting a circadian clock. *J Theor Biol*. 1970;28:327–374.
35. Mallick KS, Hajek AS, Parrish RK. Fluorouracil (5-FU) and cytarabine (ara-C) inhibition of corneal epithelial cell and conjunctival fibroblast proliferation. *Arch Ophthalmol*. 1985;103:1398–1402.
36. Moll R, Franke WW, Schiller DL, Geiger B, Krepler R. The catalog of human cytokeratins: patterns of expression in normal epithelia, tumors and cultured cells. *Cell*. 1982;31:11–24.
37. Kurpakus MA, Maniaci MT, Esco M. Expression of keratins K12, K4 and K14 during development of ocular surface epithelium. *Curr Eye Res*. 1994;13:805–814.
38. Ouyang H, Xue Y, Lin Y, et al. WNT7A and PAX6 define corneal epithelium homeostasis and pathogenesis. *Nature*. 2014;511:358–361.
39. Koroma BM, Yang JM, Sundin OH. The Pax-6 homeobox gene is expressed throughout the corneal and conjunctival epithelia. *Invest Ophthalmol Vis Sci*. 1997;38:108–120.
40. Yoshida S, Shimmura S, Kawakita T, et al. Cytokeratin 15 can be used to identify the limbal phenotype in normal and diseased ocular surfaces. *Invest Ophthalmol Vis Sci*. 2006;47:4780–4786.
41. Li Z, Burns AR, Miller SB, Smith CW. CCL20, $\gamma\delta$ T cells, and IL-22 in corneal epithelial healing. *FASEB J*. 2011;25:2659–2668.
42. Byeseda SE, Burns AR, Dieffenbaugher S, Rumbaut RE, Smith CW, Li Z. ICAM-1 is necessary for epithelial recruitment of gammadelta T cells and efficient corneal wound healing. *Am J Pathol*. 2009;175:571–579.
43. Yamagami S, Yokoo S, Usui T, Yamagami H, Amano S, Ebihara N. Distinct populations of dendritic cells in the normal human donor corneal epithelium. *Invest Ophthalmol Vis Sci*. 2005;46:4489–4494.
44. Forrester JV, Xu H, Kuffová L, Dick AD, McMenamin PG. Dendritic cell physiology and function in the eye. *Immunol Rev*. 2010;234:282–304.
45. Kofuji P, Mure LS, Massman LJ, Purrier N, Panda S, England WC. Intrinsically photosensitive retinal ganglion cells (ipRGCs) are necessary for light entrainment of peripheral clocks. *PLoS One*. 2016;11:e0168651.
46. Vigh B, Vigh-Teichmann I. Light- and electron-microscopic demonstration of immunoreactive opsin in the pinealocytes of various vertebrates. *Cell Tissue Res*. 1981;221:451–463.
47. Cavallari N, Frigato E, Vallone D, et al. A blind circadian clock in cavefish reveals that opsins mediate peripheral clock photoreception. *PLoS Biol*. 2011;9:e1001142.
48. Provencio I, Jiang G, De Grip WJ, Hayes WP, Rollag MD. Melanopsin: An opsin in melanophores, brain, and eye. *Proc Natl Acad Sci USA*. 1998;95:340–345.
49. Kojima D, Fukada Y. Non-visual photoreception by a variety of vertebrate opsins. *Novartis Found Symp*. 1999;224:265–279, discussion 279–282.

50. Foster RG, Grace MS, Provencio I, Degrip WJ, Garcia-Fernandez JM. Identification of vertebrate deep brain photoreceptors. *Neurosci Biobehav Rev.* 1994;18:541–546.
51. Provencio I, Foster RG. Vitamin A2-based photopigments within the pineal gland of a fully terrestrial vertebrate. *Neurosci Lett.* 1993;155:223–226.
52. Foster RG, Follett BK, Lythgoe JN. Rhodopsin-like sensitivity of extra-retinal photoreceptors mediating the photoperiodic response in quail. *Nature.* 1985;313:50–52.
53. Okano T, Yoshizawa T, Fukada Y. Pinopsin is a chicken pineal photoreceptive molecule. *Nature.* 1994;372:94–97.
54. Davies WI, Tamai TK, Zheng L, et al. An extended family of novel vertebrate photopigments is widely expressed and displays a diversity of function. *Genome Res.* 2015;25:1666–1679.
55. Dalesio NM, Barreto Ortiz SF, Pluznick JL, Berkowitz DE. Olfactory, taste, and photo sensory receptors in non-sensory organs: it just makes sense. *Front Physiol.* 2018;9:1673.
56. de Assis LVM, Moraes MN, Magalhães-Marques KK, Castrucci AML. Melanopsin and rhodopsin mediate UVA-induced immediate pigment darkening: unravelling the photosensitive system of the skin. *Eur J Cell Biol.* 2018;97:150–162.
57. Tarttelin EE, Bellingham J, Hankins MW, Foster RG, Lucas RJ. Neuropsin (Opn5): a novel opsin identified in mammalian neural tissue. *FEBS Lett.* 2003;554:410–416.
58. Blackshaw S, Snyder SH. Encephalopsin: a novel mammalian extraretinal opsin discretely localized in the brain. *J Neurosci.* 1999;19:3681–3690.
59. Nayak G, Zhang KX, Vemaraju S, et al. Adaptive thermogenesis in mice is enhanced by opsin 3-dependent adipocyte light sensing. *Cell Rep.* 2020;30:672–686.e678.
60. Sikka G, Hussmann GP, Pandey D, et al. Melanopsin mediates light-dependent relaxation in blood vessels. *Proc Natl Acad Sci USA.* 2014;111:17977–17982.
61. Barreto Ortiz S, Hori D, Nomura Y, et al. Opsin 3 and 4 mediate light-induced pulmonary vasorelaxation that is potentiated by G protein-coupled receptor kinase 2 inhibition. *Am J Physiol Lung Cell Mol Physiol.* 2018;314:L93–L106.
62. Xue T, Do MT, Riccio A, et al. Melanopsin signalling in mammalian iris and retina. *Nature.* 2011;479:67–73.
63. Tsuchiya S, Buhr ED, Higashide T, Sugiyama K, Van Gelder RN. Light entrainment of the murine intraocular pressure circadian rhythm utilizes non-local mechanisms. *PLoS One.* 2017;12:e0184790.
64. Sato M, Tsuji T, Yang K, et al. Cell-autonomous light sensitivity via Opsin3 regulates fuel utilization in brown adipocytes. *PLoS Biol.* 2020;18:e3000630.
65. Tsutsumi M, Ikeyama K, Denda S, et al. Expressions of rod and cone photoreceptor-like proteins in human epidermis. *Exp Dermatol.* 2009;18:567–570.
66. Haltaufderhyde K, Ozdeslik RN, Wicks NL, Najera JA, Oancea E. Opsin expression in human epidermal skin. *Photochem Photobiol.* 2015;91:117–123.
67. Kusumoto J, Takeo M, Hashikawa K, et al. OPN4 belongs to the photosensitive system of the human skin. *Genes Cells.* 2020;25:215–225.
68. Delwig A, Larsen DD, Yasumura D, Yang CF, Shah NM, Copenhagen DR. Retinofugal projections from melanopsin-expressing retinal ganglion cells revealed by intraocular injections of Cre-dependent virus. *PLoS One.* 2016;11:e0149501.
69. Hoyle NP, Seinkmane E, Putker M, et al. Circadian actin dynamics drive rhythmic fibroblast mobilization during wound healing. *Sci Transl Med.* 2017;9:eaal2774.
70. Sandvig KU, Haaskjold E, Refsum SB. Time dependency in the regenerative response to injury of the rat corneal epithelium. *Chronobiol Int.* 1994;11:173–179.
71. Kuffler DP. Photobiomodulation in promoting wound healing: a review. *Regen Med.* 2016;11:107–122.